

# Optical Remote Sensing with Differential Absorption Lidar (DIAL)

Christoph Senff

CIRES, University of Colorado &  
NOAA/ESRL/CSD/Atmospheric Remote Sensing Group

<http://www.etl.noaa.gov/et2>

Guest lecture for ASEN-6519 Lidar Remote Sensing  
CU Boulder

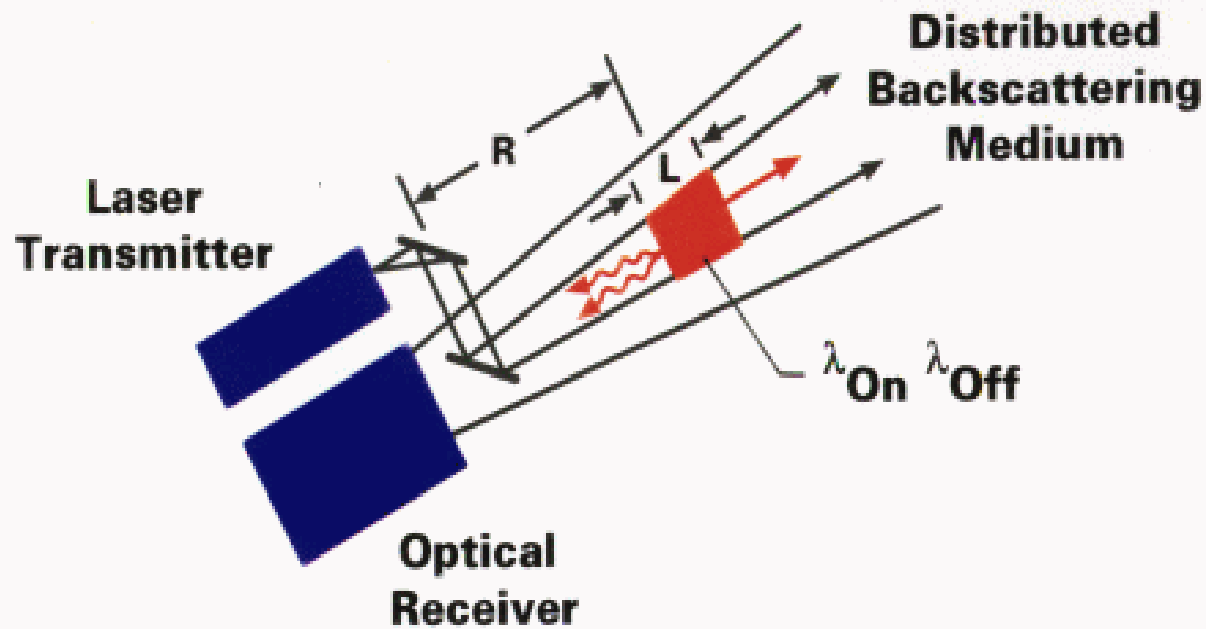
November 3, 2008

# Outline

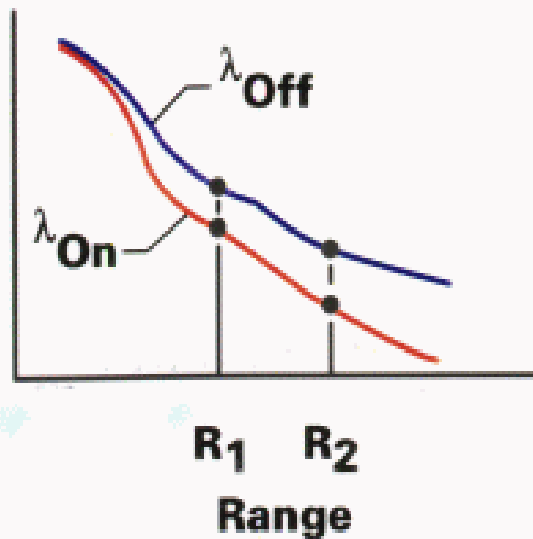
---

- **DIAL concept**
- **A short history of DIAL**
- **DIAL equation, error analysis, and system components**
- **DIAL systems at NOAA/ESRL/CSD**
- **Multi-wavelength ozone DIAL**
- **Applications of airborne ozone DIAL**

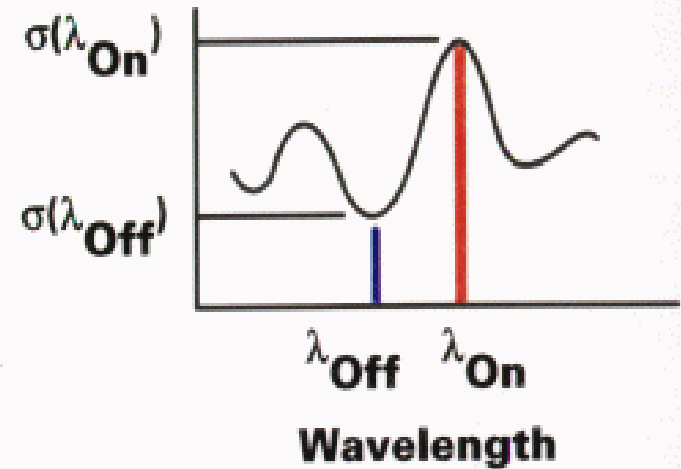
# Differential Absorption Lidar (DIAL) Concept



Power Received,  
 $P_r$



Absorption  
Cross  
Section



# Atmospheric gases measured with DIAL

---

- H<sub>2</sub>O
- O<sub>3</sub>
- SO<sub>2</sub>
- NO<sub>2</sub>, NO
- NH<sub>3</sub>
- CH<sub>4</sub>
- CO<sub>2</sub>
- Hg
- VOCs (Volatile Organic Compounds)
- Toluene
- Benzene

# First DIAL measurements

---

Richard M. Schotland (“The father of DIAL”)

1964 – Measured vertical profiles of water vapor by thermally tuning a ruby laser on and off the water vapor absorption line at 694.38 nm.

Only 4 years after invention of ruby lidar!

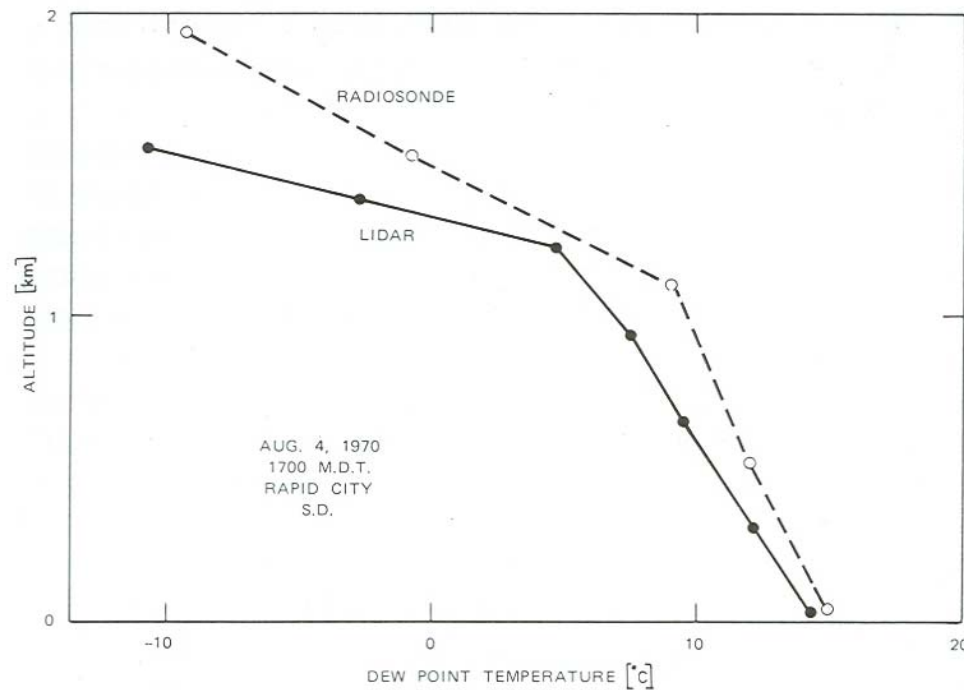
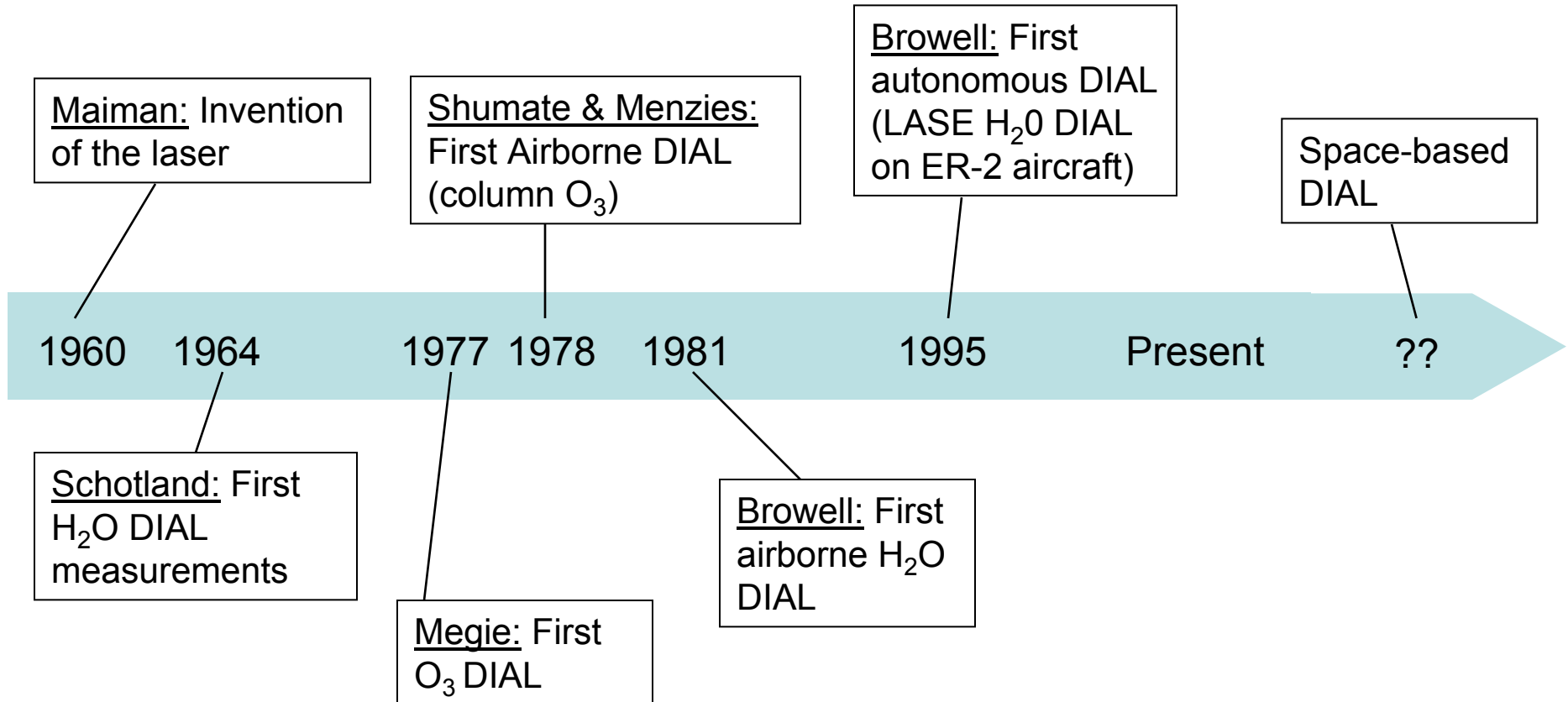


Fig. 4.20. Comparison of atmospheric water vapor vertical profiles (expressed as dew point temperature) measured by differential absorption lidar and radiosonde [4.82]

# Major milestones in the history of DIAL

---



# DIAL equation

---

Single scattering, elastic backscatter LIDAR equation:

$$N_S(\lambda, R) = N_L(\lambda) [\beta(\lambda, R)\Delta R] \frac{A}{R^2} \exp\left[-2\int_0^R \alpha(\lambda, r) dr\right] [\eta(\lambda) G(\lambda, R)] + N_B(\lambda)$$

Ratio LIDAR equations for online and offline wavelengths  $\lambda_{on}$  and  $\lambda_{off}$  :

$$\begin{aligned} \frac{N_S(\lambda_{off}, R) - N_B(\lambda_{off}, R)}{N_S(\lambda_{on}, R) - N_B(\lambda_{on}, R)} &= \frac{N_L(\lambda_{off}) \eta(\lambda_{off}) G(\lambda_{off}, R) \beta(\lambda_{off}, R)}{N_L(\lambda_{on}) \eta(\lambda_{on}) G(\lambda_{on}, R) \beta(\lambda_{on}, R)} \\ &\times \exp\left[-2\int_0^R \alpha(\lambda_{off}, r) - \alpha(\lambda_{on}, r) dr\right] \quad \boxed{\text{Number density of constituent C}} \\ &\times \exp\left[-2\int_0^R (\sigma_C(\lambda_{off}, r) - \sigma_C(\lambda_{on}, r)) n_C(r) dr\right] \\ &\times \exp\left[-2\int_0^R \sum_{i=1}^m [(\sigma_{X_i}(\lambda_{off}, r) - \sigma_{X_i}(\lambda_{on}, r)) n_{X_i}(r)] dr\right] \end{aligned}$$

## DIAL equation (cont'd)

---

$$\begin{aligned}
 n_C = & \frac{1}{2 \Delta \sigma_C(R)} \frac{d}{dR} \ln \left[ \frac{N_S(\lambda_{off}, R) - N_B(\lambda_{off})}{N_S(\lambda_{on}, R) - N_B(\lambda_{on})} \right] \\
 & - \frac{1}{2 \Delta \sigma_C(R)} \frac{d}{dR} \ln \frac{G(\lambda_{off}, R)}{G(\lambda_{on}, R)} \quad [G] \\
 & - \frac{1}{2 \Delta \sigma_C(R)} \frac{d}{dR} \ln \frac{\beta(\lambda_{off}, R)}{\beta(\lambda_{on}, R)} \quad [B] \\
 & - \frac{1}{\Delta \sigma_C(R)} [\alpha(\lambda_{on}, R) - \alpha(\lambda_{off}, R)] \quad [E] \\
 & - \frac{1}{\Delta \sigma_C(R)} \sum_{i=1}^m \Delta \sigma_{X_i}(R) n_{X_i}(R) \quad [X]
 \end{aligned}$$

*with*  $\Delta \sigma_C(R) = \sigma_C(\lambda_{on}, R) - \sigma_C(\lambda_{off}, R)$

G = differential geometrical factor

E = differential extinction

B = differential backscatter

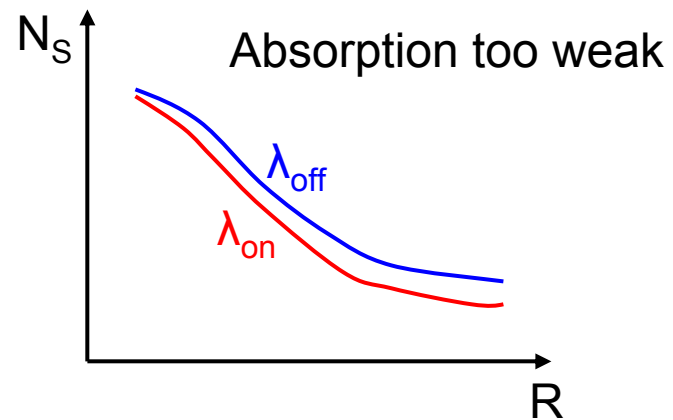
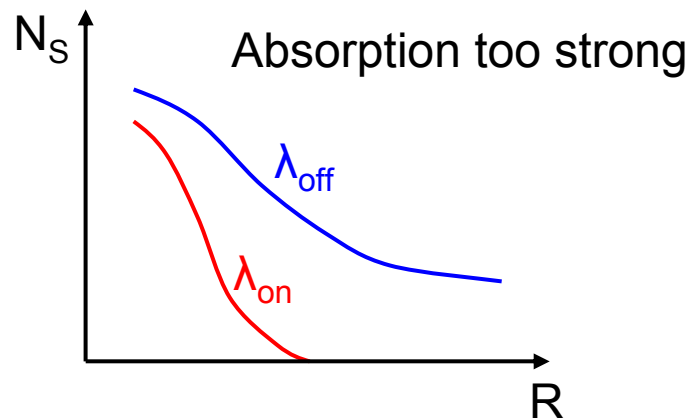
X = interfering constituents



# How to choose an appropriate absorption line for DIAL

$$N_S(\lambda_{on}, R) \propto \exp \left[ -2 \int_0^R \sigma_C(\lambda_{on}, r) n_C(r) dr \right]$$

Extinction of online wavelength due to absorption by constituent C must be neither too small or too large.



Best precision in  $n_C$  when:  $\tau(\lambda_{on}, R_{\max}) = \int_0^{R_{\max}} \sigma_C(\lambda_{on}, r) n_C(r) dr = 1.1$

Example:  $mr_{O_3} = 80 \text{ ppb} \Rightarrow n_{O_3} = 2 \times 10^{18} \text{ m}^{-3}, R_{\max} = 3 \text{ km}$

$$\sigma_{O_3}(\lambda_{on}) n_{O_3} R_{\max} = 1.1 \Rightarrow \sigma_{O_3}(\lambda_{on}) = 1.83 \times 10^{-22} \text{ m}^2$$

## Precision of DIAL measurements

Simple “back of the envelope” calculation:

$$n_c = \frac{1}{2 \Delta \sigma_c(R) \Delta R} \ln \left[ \frac{N(\lambda_{off}, R + \Delta R) N(\lambda_{on}, R)}{N(\lambda_{on}, R + \Delta R) N(\lambda_{off}, R)} \right] \quad \text{with } N = N_S - N_B$$

$$\delta n_c = \frac{1}{2 \Delta \sigma_c(R) \Delta R} \sqrt{\sum_{i,j} \frac{\delta^2(N(\lambda_i, R_j))}{(N(\lambda_i, R_j))^2}} \approx \frac{1}{\Delta \sigma_c \Delta R} \frac{\delta N}{N} = \frac{1}{\Delta \sigma_c \Delta R SNR}$$

$$\frac{\delta n_c}{n_c} = \frac{1}{\tau_{\Delta R} SNR} \Rightarrow \boxed{SNR = \frac{1}{\tau_{\Delta R} \delta n_c / n_c}}$$

$$\text{Example: } \tau_{\Delta R} = 0.05, \delta n_c / n_c = 5\% \Rightarrow \boxed{SNR = 400!}$$

Even modest precision of 5% requires high SNR. SNR can be increased by averaging on/offline signals time- and range-wise.

$$\text{Poisson statistics: } \delta N = N^{0.5} \Rightarrow SNR = N^{0.5}$$

$$\text{Since } N \propto \Delta t \Delta R, \boxed{SNR \propto \Delta t^{0.5} \Delta R^{0.5} \text{ and } \delta n_c \propto \Delta t^{-0.5} \Delta R^{-1.5}}$$

# Accuracy of DIAL measurements

$$n_C = \frac{1}{2\Delta\sigma_C(R)} \frac{d}{dR} \ln \left[ \frac{N_S(\lambda_{off}, R) - N_B(\lambda_{off})}{N_S(\lambda_{on}, R) - N_B(\lambda_{on})} \right]$$

$$- \frac{1}{2\Delta\sigma_C(R)} \frac{d}{dR} \ln \frac{G(\lambda_{off}, R)}{G(\lambda_{on}, R)} \quad [G]$$

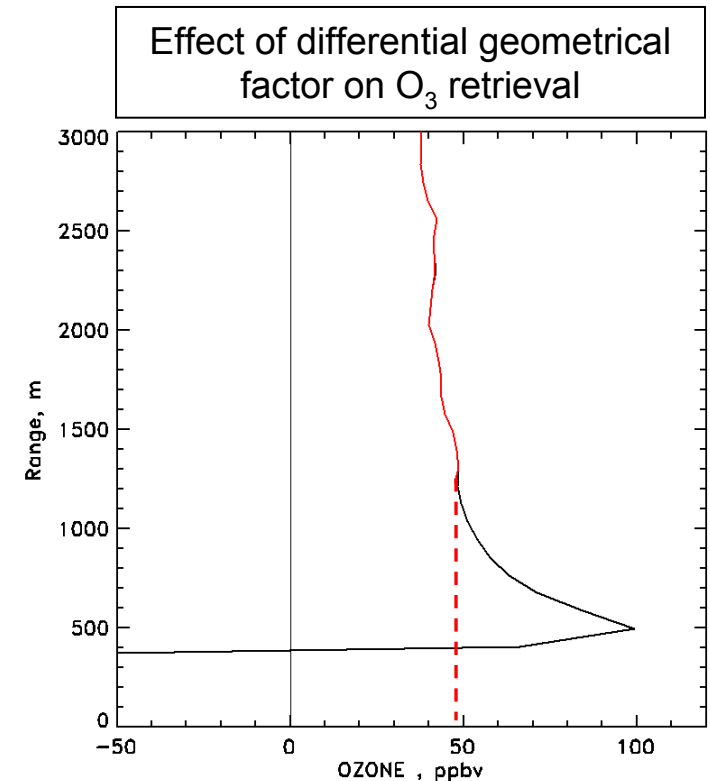
$$- \frac{1}{2\Delta\sigma_C(R)} \frac{d}{dR} \ln \frac{\beta(\lambda_{off}, R)}{\beta(\lambda_{on}, R)} \quad [B]$$

$$- \frac{1}{\Delta\sigma_C(R)} [\alpha(\lambda_{on}, R) - \alpha(\lambda_{off}, R)] \quad [E]$$

$$- \frac{1}{\Delta\sigma_C(R)} \sum_{i=1}^m \Delta\sigma_{X_i}(R) n_{X_i}(R) \quad [X]$$

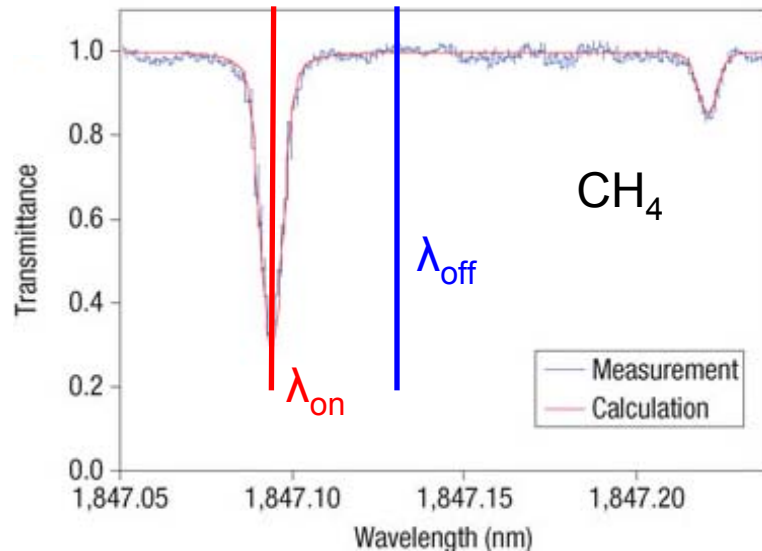
## Accuracy affected by:

- How well is absorption cross section known?
- Improper correction of signal offsets, e.g. background light
- Geometrical factor different for  $\lambda_{on}$  and  $\lambda_{off}$
- Differential backscatter & extinction not properly corrected
- Interfering species not taken into account



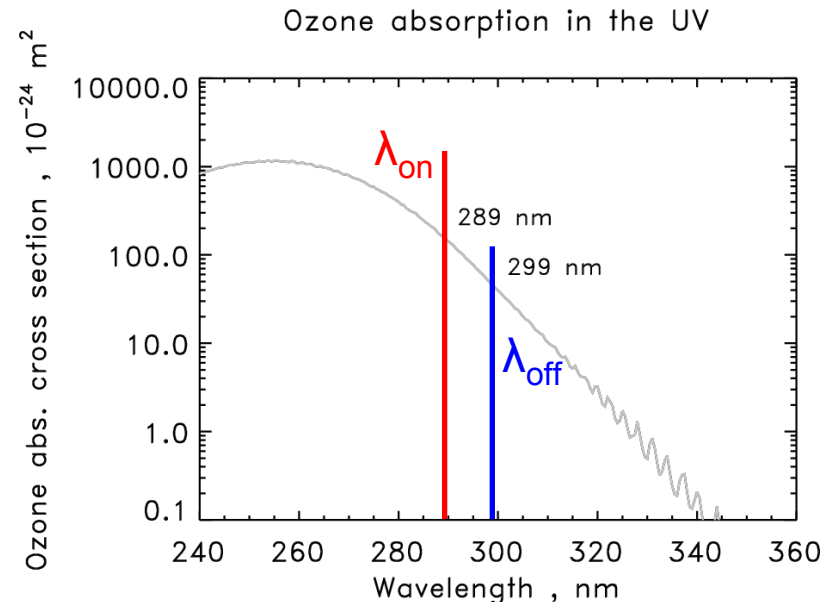
# Narrow and broad absorption lines

## Narrow absorption line



- $\Delta\lambda \approx 50 \text{ pm}$
- No correction for differential backscatter or extinction needed
- Transmit laser needs to be tunable
- High frequency stability & spectral purity

## Broad absorption feature



- $\Delta\lambda = 10 \text{ nm}$
- Correction for differential backscatter or extinction necessary
- Fixed wavelength lasers OK
- High frequency stability & spectral purity not needed

# DIAL system components

---

## LIDAR transmitter

- ❑ High power (high pulse energy or lower pulse energy & high rep rate)
- ❑ Tunable laser or appropriate fixed frequencies

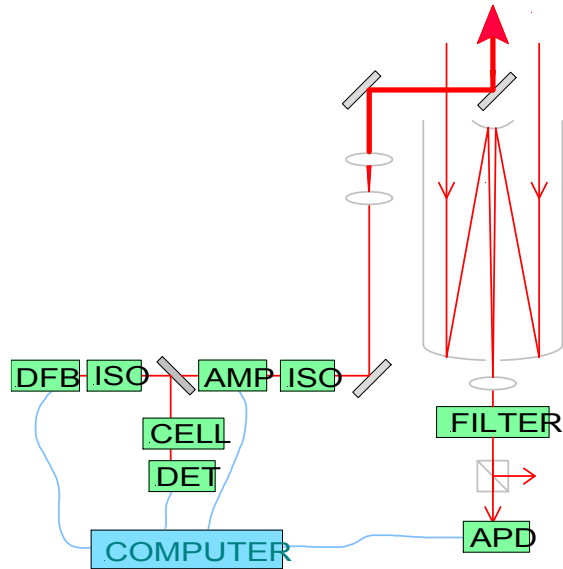
Species	Laser transmitter	Wavelengths
O <sub>3</sub>	4x Nd:YAG / Excimer + Raman shift OPO, CeLiCAF, 3x Ti:Sapphire	Fixed: 266 – 359 nm Tunable: 280 – 320 nm
H <sub>2</sub> O	Ti:Sapphire, Alexandrite, OPO, Fiber laser	720 – 940 nm, 1.5 μm
CH <sub>4</sub>	OPO	1.67 μm, 3.3 μm
CO <sub>2</sub>	Fiber laser, OPO, Tm:Ho:YLF	1.57 μm, 2.05 μm
VOCS	Dye lasers	Mid-IR @ several μm
NH <sub>3</sub>	Dye laser, CO <sub>2</sub> laser	208 nm, 9 – 10 μm

OPO = Optical Parametric Oscillator

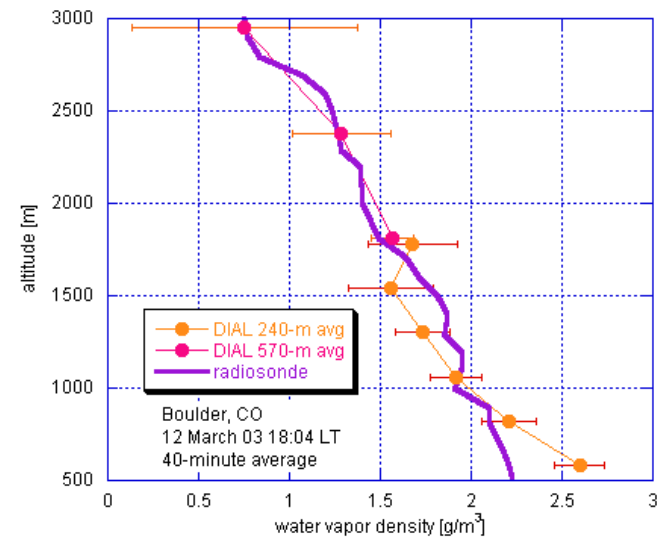


# DIALs at NOAA/ESRL/CSD – Ground-based

CODI = **CO**mpact **DIAL** (prototype of small, autonomous DIAL system)



wavelength	823 nm
output pulse energy	~0.15 $\mu$ J
pulse duration	600 ns
pulse repetition freq.	8 – 10 kHz
telescope diameter	34 cm
field-of-view	180 $\mu$ Rad



# DIALs at NOAA/ESRL/CSD - Shipborne

OPAL = Ozone Profiling Atmospheric Lidar (recently retired)

- Wavelengths: 266, 289, 299 nm
- 4x Nd:YAG + Raman-shifting in H2 and D2
- Motion-compensated elevation angle scanner from 0 – 90 deg
- Ship deployments on NOAA R/V Ron Brown in 2002 - 2006

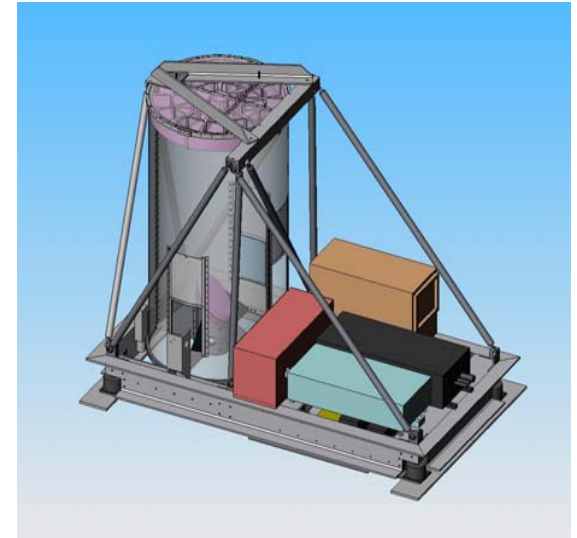




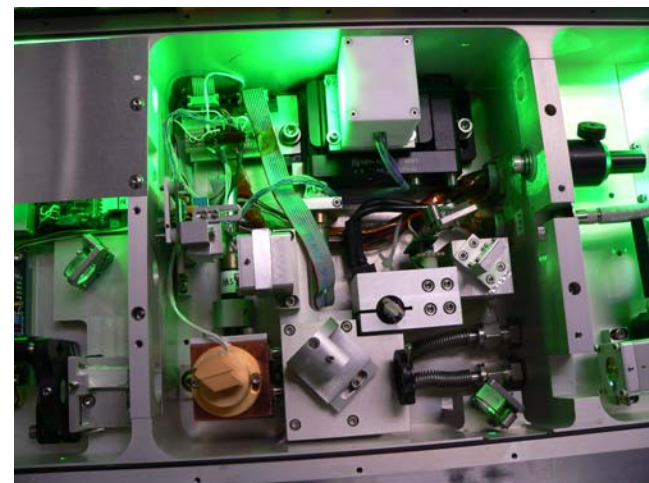
# DIALs at NOAA/ESRL/CSD - Airborne

TOPAZ = Tunable Optical Profiler of Aerosol and oZone

- Tunable, all-solid state, compact airborne O<sub>3</sub> DIAL
- Replaced previous fixed-wavelength O<sub>3</sub> lidar in 2006
- Size & weight were reduced significantly

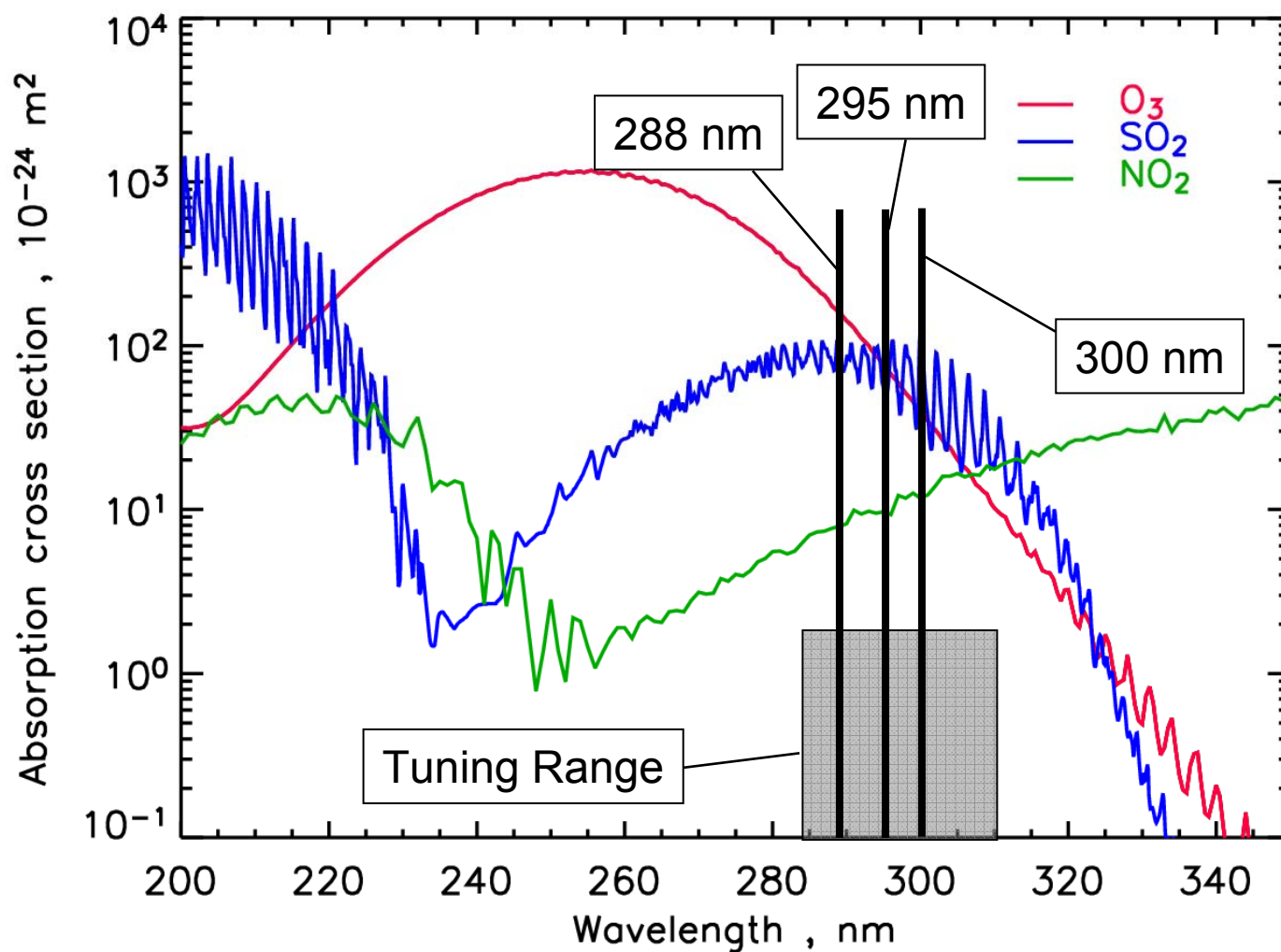


TOPAZ Specifications	
Wavelengths	3
Wavelength tuning range	285-310 nm
Pulse energy	0.2-0.8 mJ/pulse
Pulse rate	1 kHz with pulse-to-pulse tuning capability
Minimum/maximum range	0.3 km / 4 km
Eye-safe range	~150 m
System weight	~800 lbs (including chiller and control electronics)
Output	Ozone and aerosol backscatter profiles
Vertical/horizontal resolution	90 m / 600 m
Precision	3 - 15 ppb





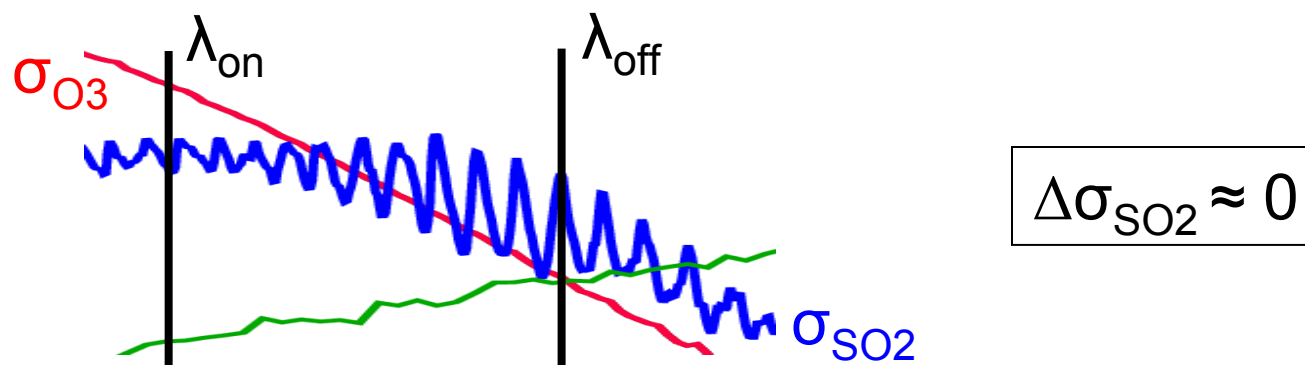
# TOPAZ wavelengths & tuning range



# TOPAZ is a tunable, multi-wavelength DIAL system

## Advantages of tunability:

- Wavelengths can be optimized for given atmospheric ozone loading
- Minimize interference from other trace gases, e.g. SO<sub>2</sub>



## Advantages of multi-wavelength capability:

- Allows simultaneous measurement of 2 species (O<sub>3</sub> & SO<sub>2</sub>)
- Dual-DIAL application to minimize uncertainties due to aerosol backscatter and extinction corrections

Dual-DIAL = 2 DIAL wavelength pairs, i.e. 288/295 nm & 295/300 nm

# Back to single-DIAL ozone retrieval for a moment

$$n_c = \frac{1}{2 \Delta \sigma_c(R)} \frac{d}{dR} \ln \left[ \frac{N_S^*(\lambda_{off}, R)}{N_S^*(\lambda_{on}, R)} \right]$$

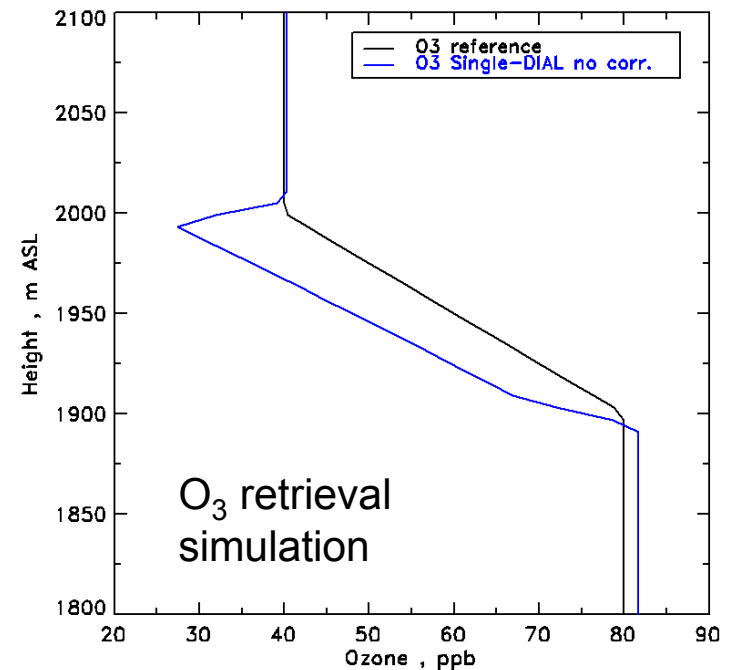
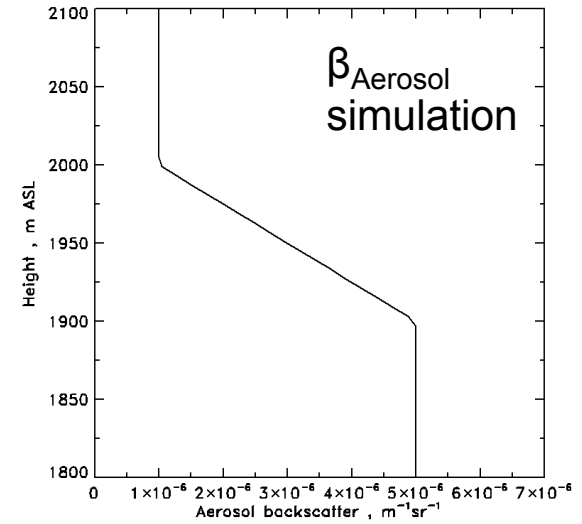
$$- \frac{1}{2 \Delta \sigma_c(R)} \frac{d}{dR} \ln \frac{\beta(\lambda_{off}, R)}{\beta(\lambda_{on}, R)} \quad [B]$$

$$- \frac{1}{\Delta \sigma_c(R)} [\alpha(\lambda_{on}, R) - \alpha(\lambda_{off}, R)] \quad [E]$$

$$\beta = \beta_{Rayleigh} + \beta_{Aerosol}, \quad \alpha = \alpha_{Rayleigh} + \alpha_{Aerosol}$$

$\beta_{Aerosol}$  and  $\alpha_{Aerosol}$  have to be determined from offline signal data and wavelength dependence of  $\beta$  and  $\alpha$  have to be guessed.

Lots of potential to introduce errors in  $O_3$  retrieval!



## Dual-DIAL minimizes aerosol interference

---

$$\begin{aligned}
 n_C = & \frac{1}{2 \delta \sigma_C(R)} \frac{d}{dR} \left[ \ln \frac{N_S^*(\lambda_{off1}, R)}{N_S^*(\lambda_{on1}, R)} - C \ln \frac{N_S^*(\lambda_{off2}, R)}{N_S^*(\lambda_{on2}, R)} \right] \\
 & - \frac{1}{2 \delta \sigma_C(R)} \frac{d}{dR} \left[ \ln \frac{\beta(\lambda_{off1}, R)}{\beta(\lambda_{on1}, R)} - C \ln \frac{\beta(\lambda_{off2}, R)}{\beta(\lambda_{on2}, R)} \right] \quad [B'] \\
 & - \frac{1}{\delta \sigma_C(R)} \left[ \alpha(\lambda_{on1}, R) - \alpha(\lambda_{off1}, R) - C \left( \alpha(\lambda_{on2}, R) - \alpha(\lambda_{off2}, R) \right) \right] \quad [E']
 \end{aligned}$$

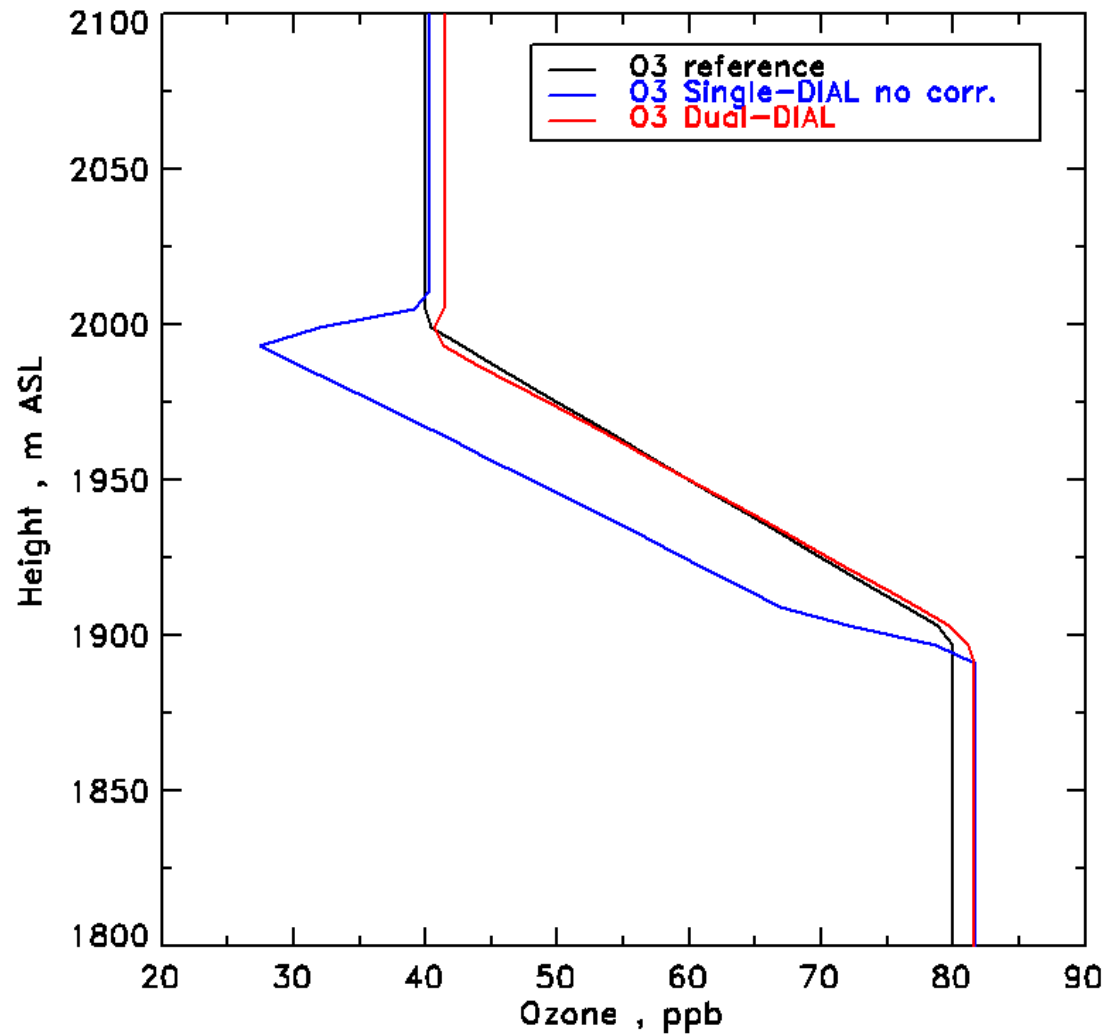
with  $\delta \sigma_C(R) = \Delta \sigma_{C1} - C \Delta \sigma_{C2}$ , DIAL pair 1:  $\lambda_{on1} / \lambda_{off1}$ , DIAL pair 2:  $\lambda_{on2} / \lambda_{off2}$

$$B' = E' \approx 0 \quad \text{for} \quad C = \frac{\lambda_{on1} - \lambda_{off1}}{\lambda_{on2} - \lambda_{off2}}$$

- No correction of differential aerosol effects needed and residual errors are small.
- However, precision of DIAL retrieval is degraded.

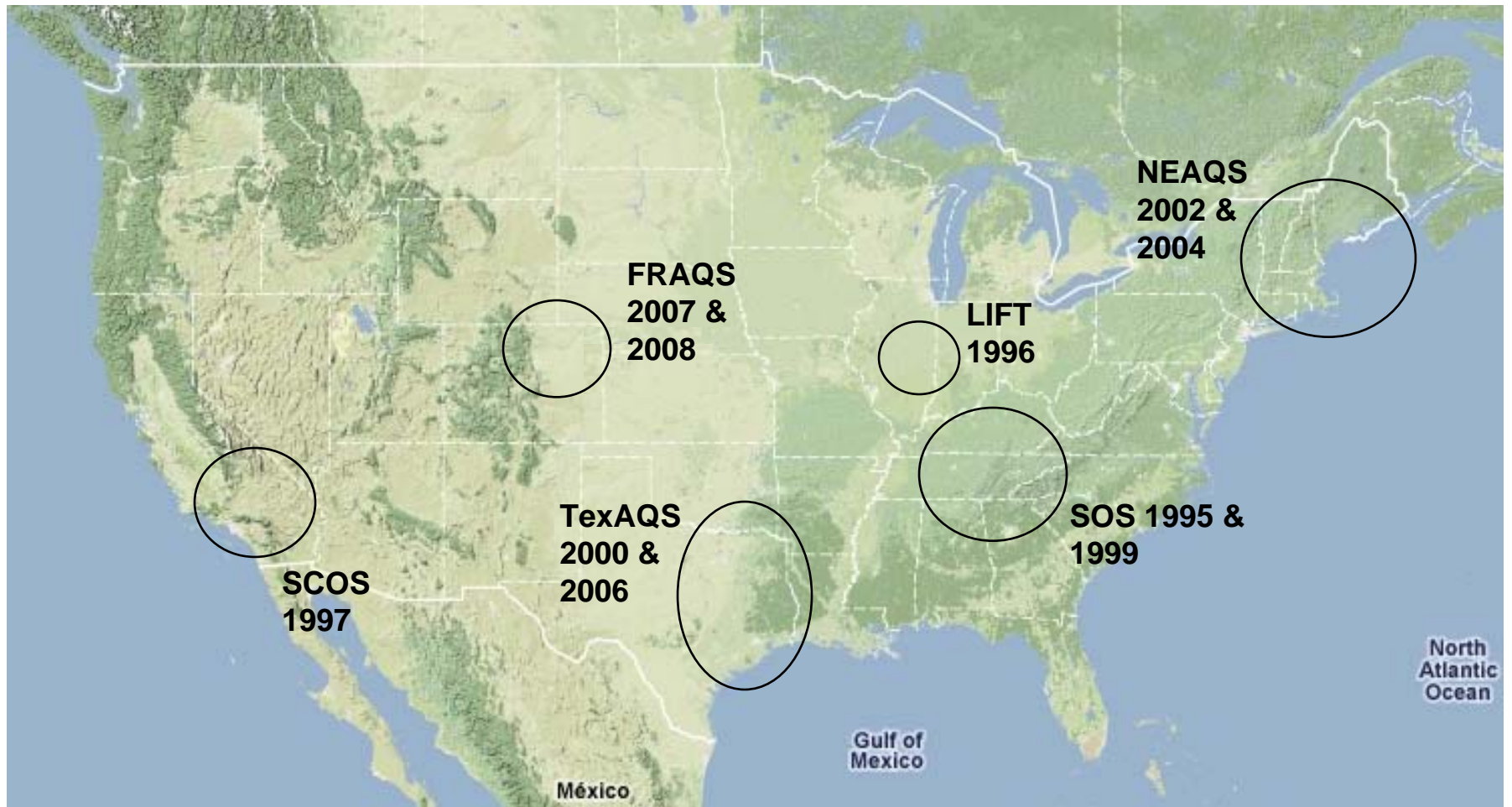
## Dual-DIAL minimizes aerosol interference (cont'd)

---



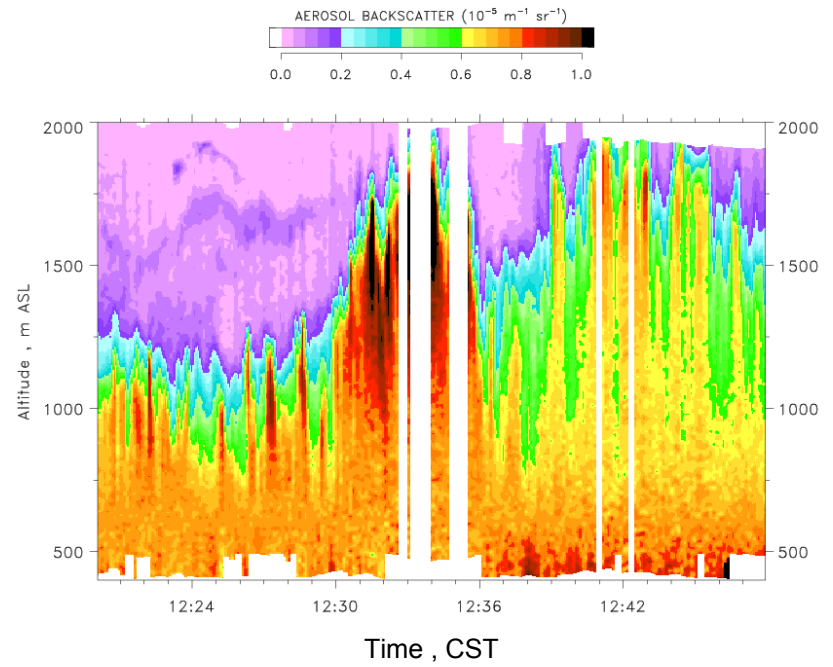
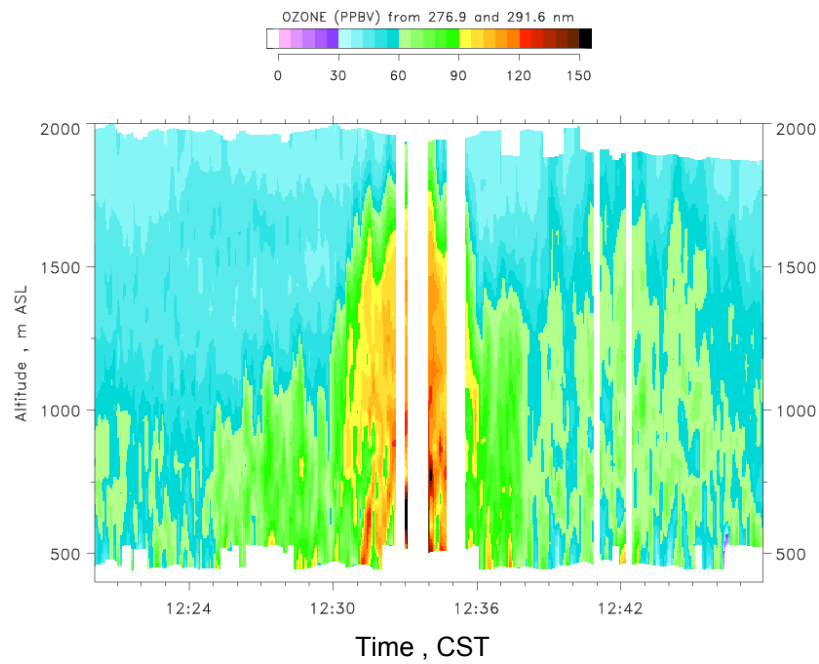
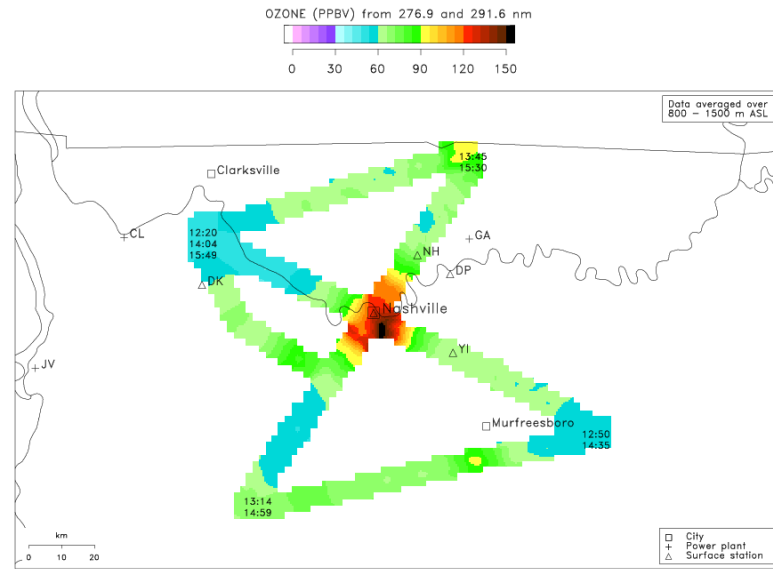
O<sub>3</sub> retrieval simulation

# Ozone DIAL Application: Regional Air Quality

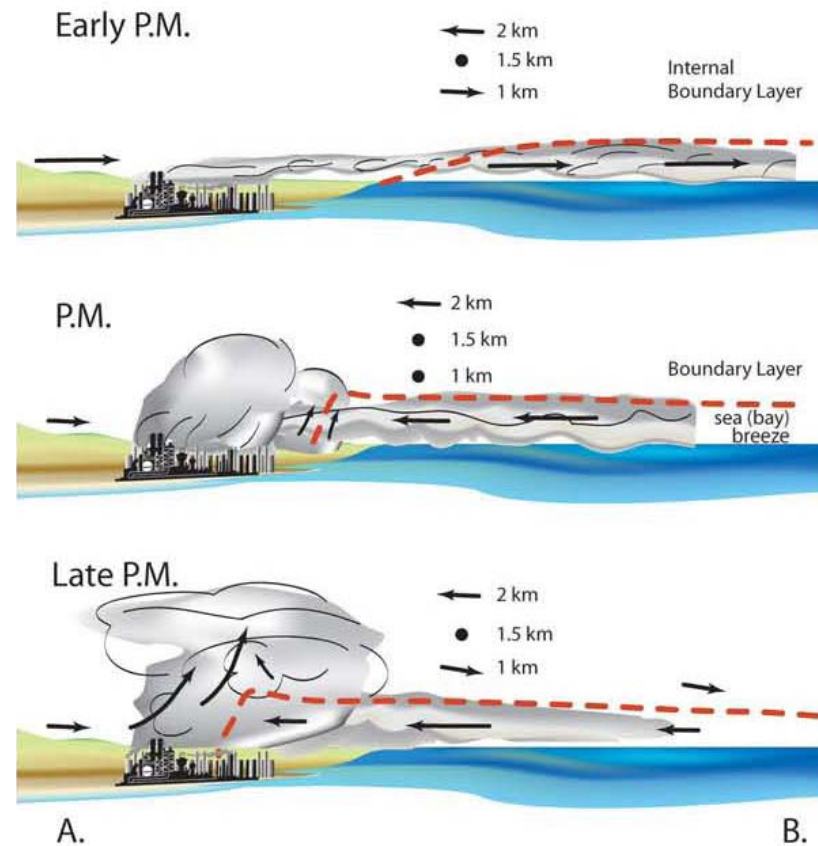
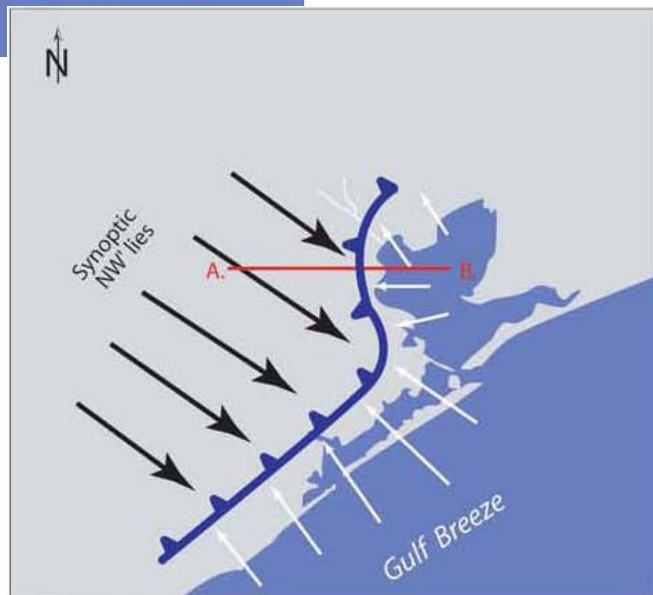




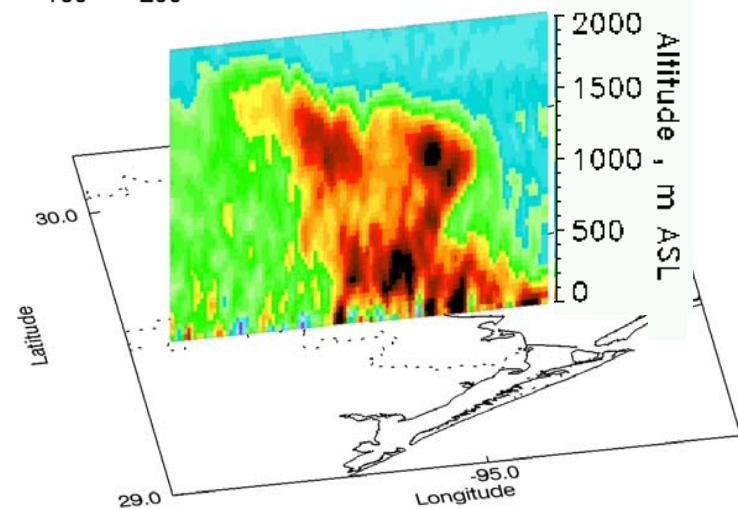
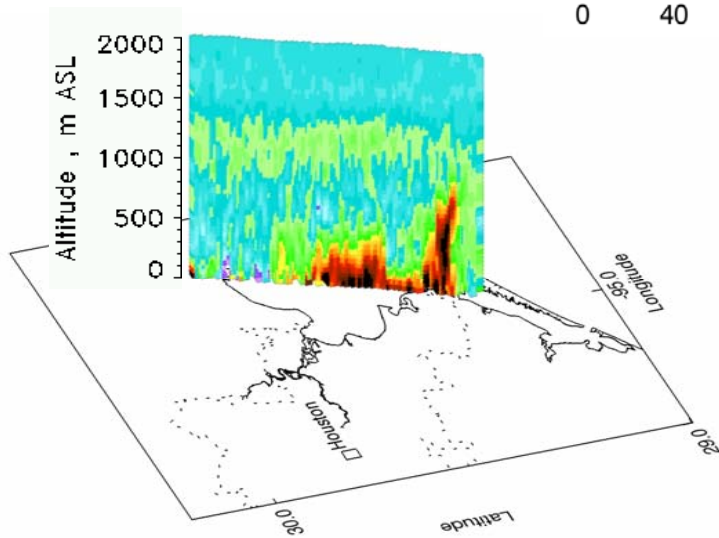
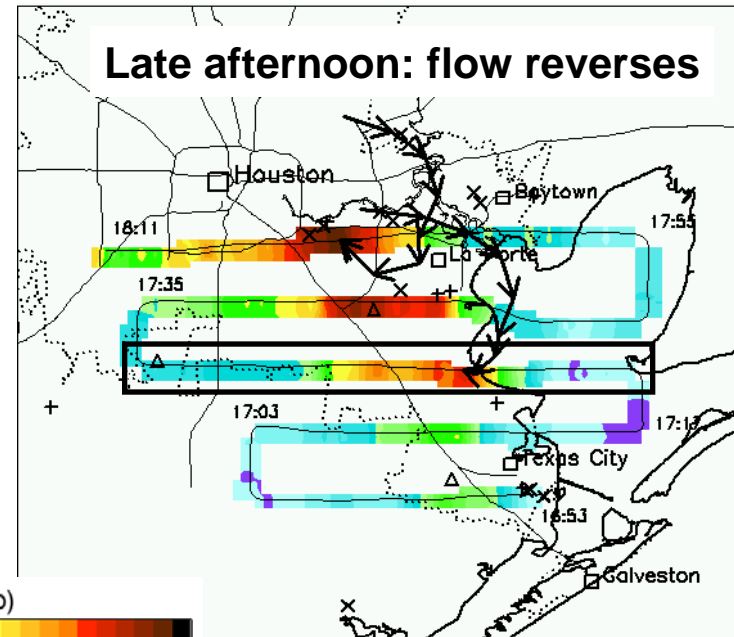
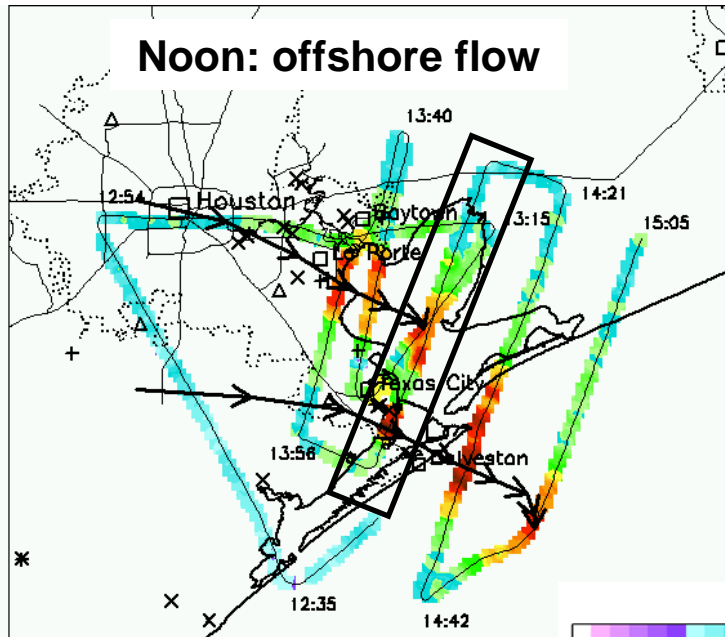
# Nashville urban plume



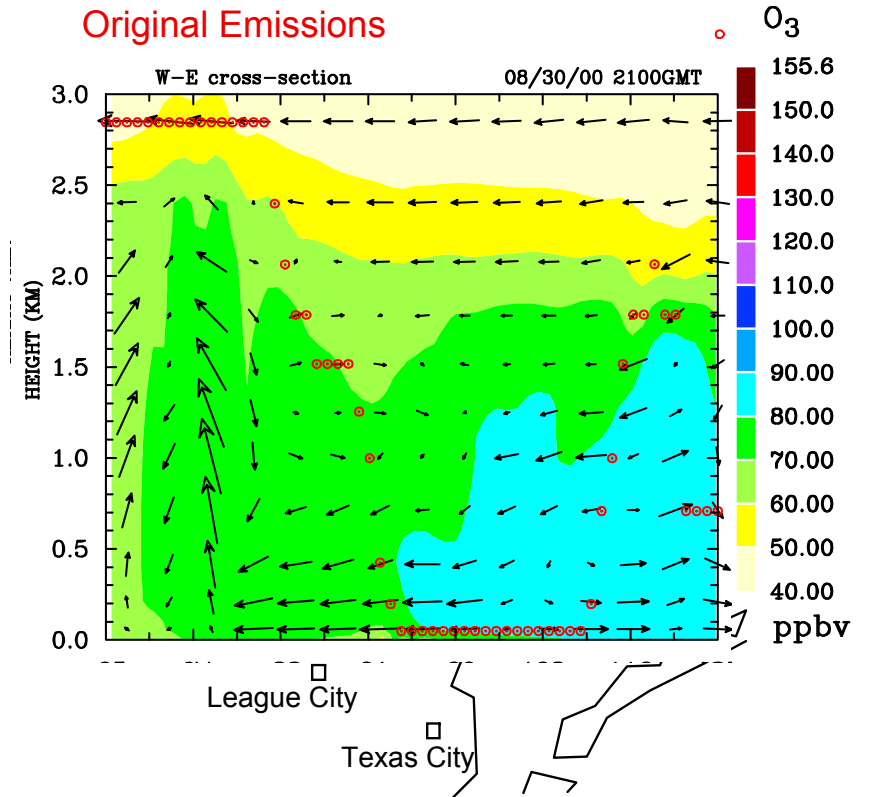
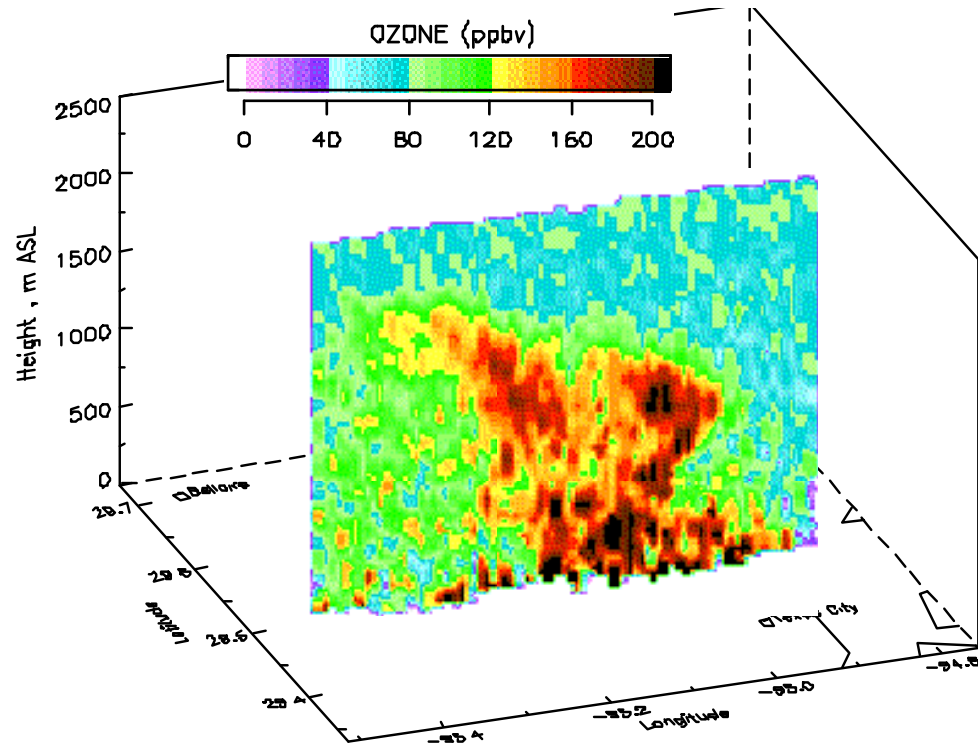
# Houston, TX: High ozone event due to sea-breeze re-circulation of pollutants



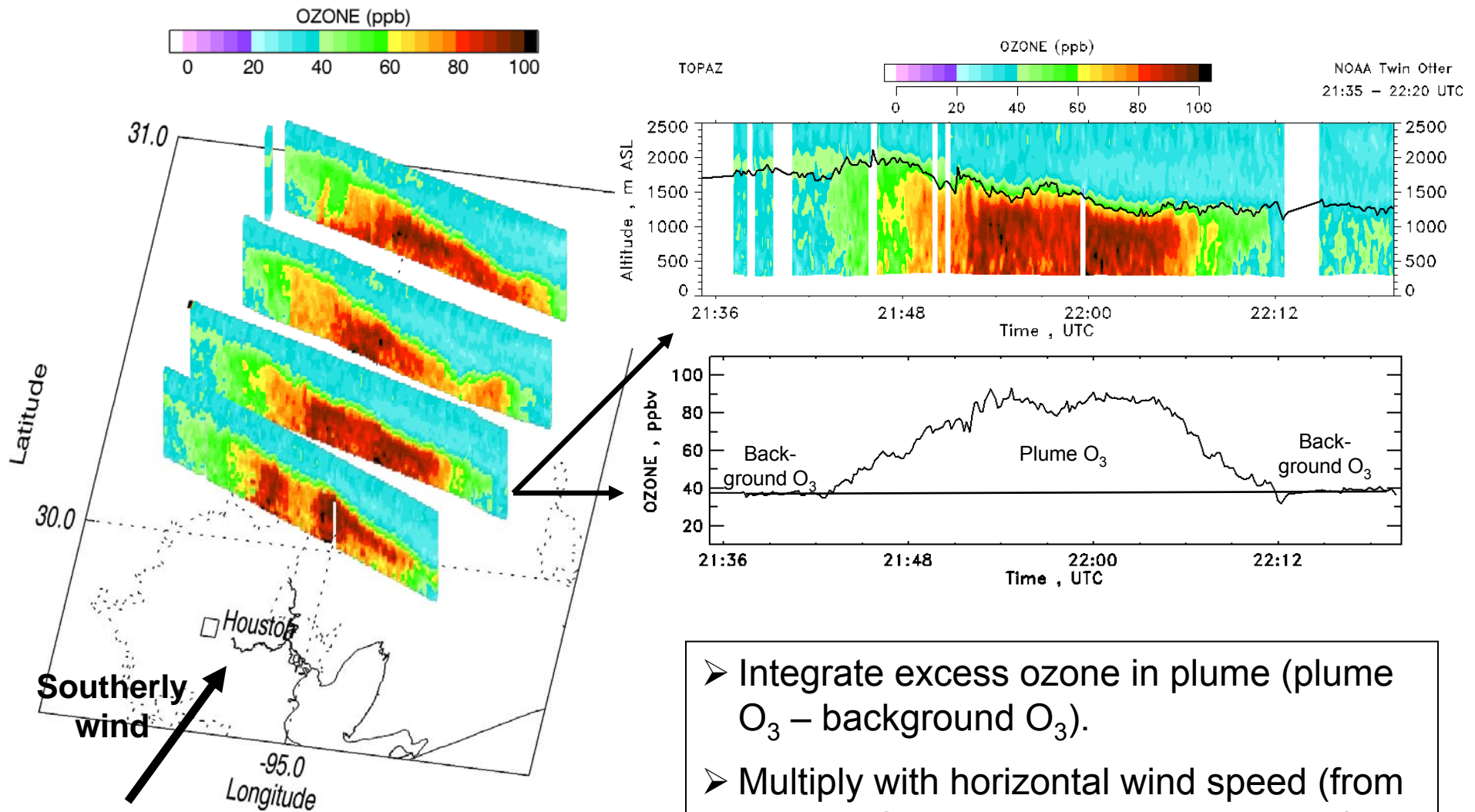
# Local Transport: Houston land-sea breeze recirculation



# AQ forecast model comparison with lidar

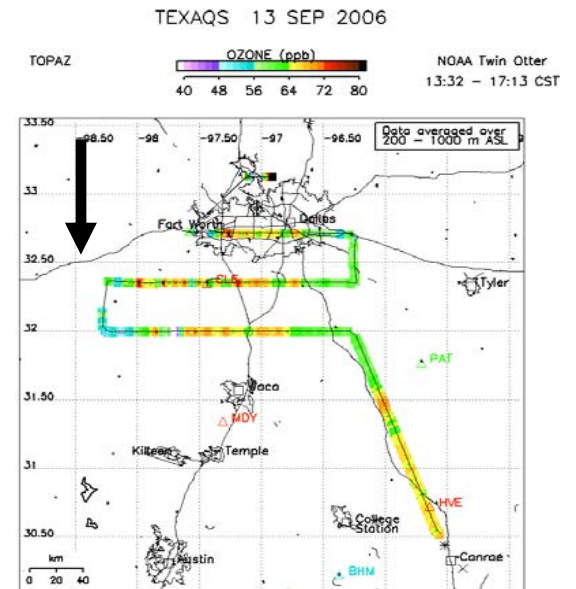
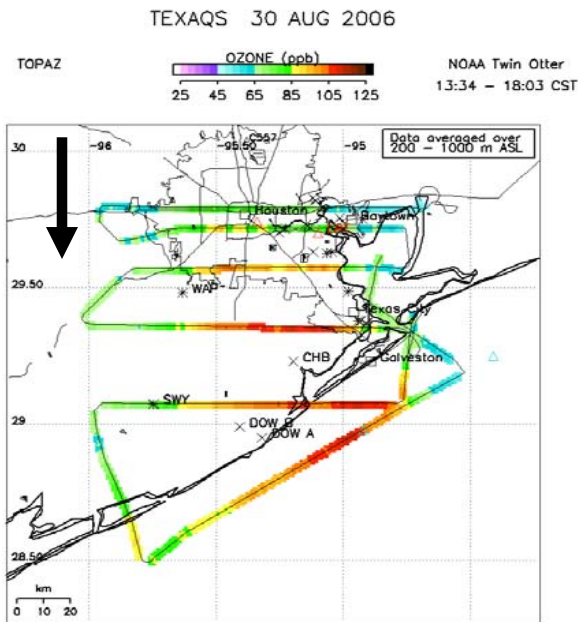
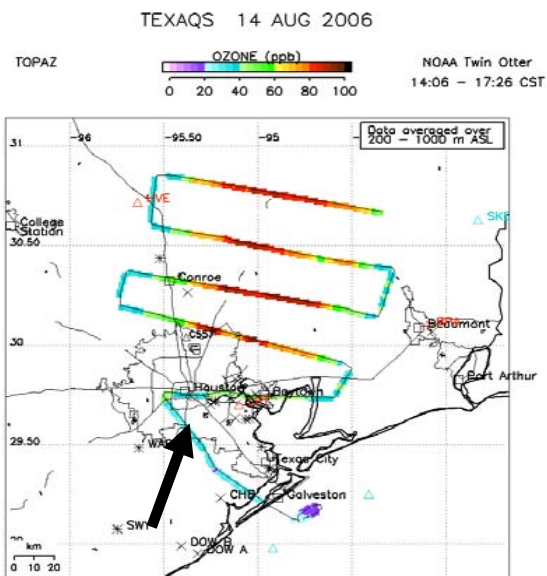
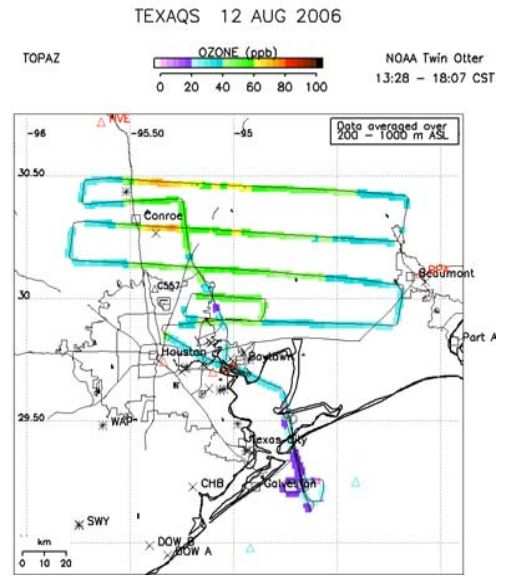
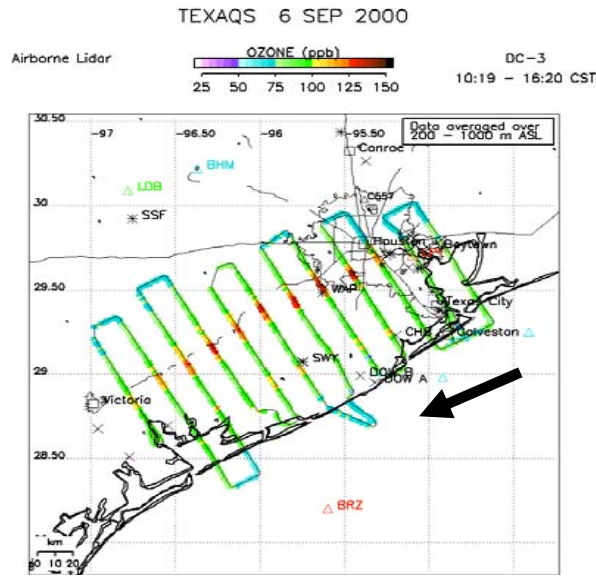
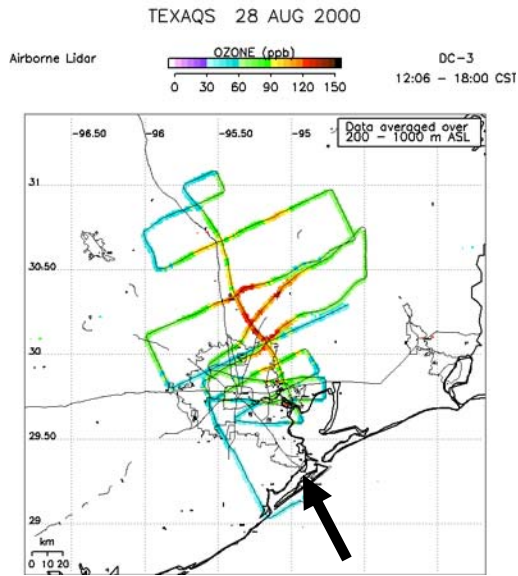


# Regional Transport: Estimating ozone exported from Houston



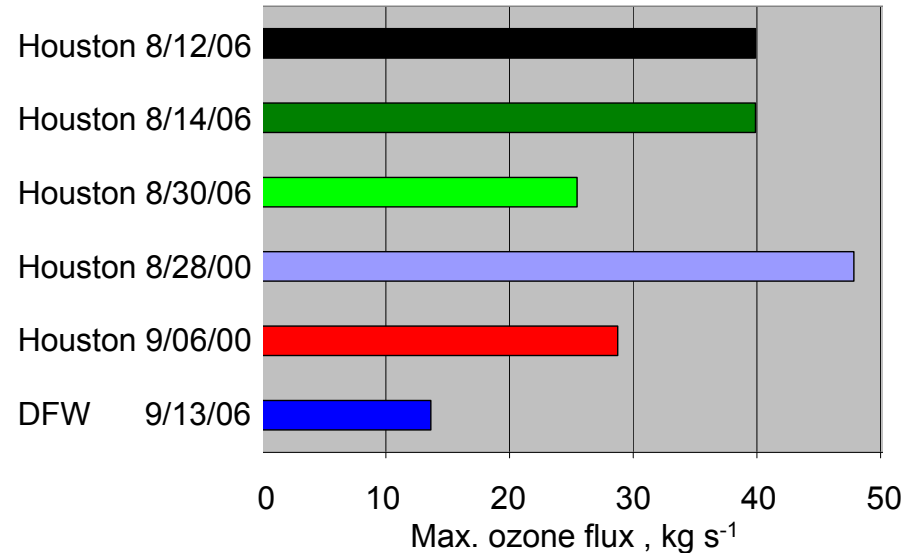
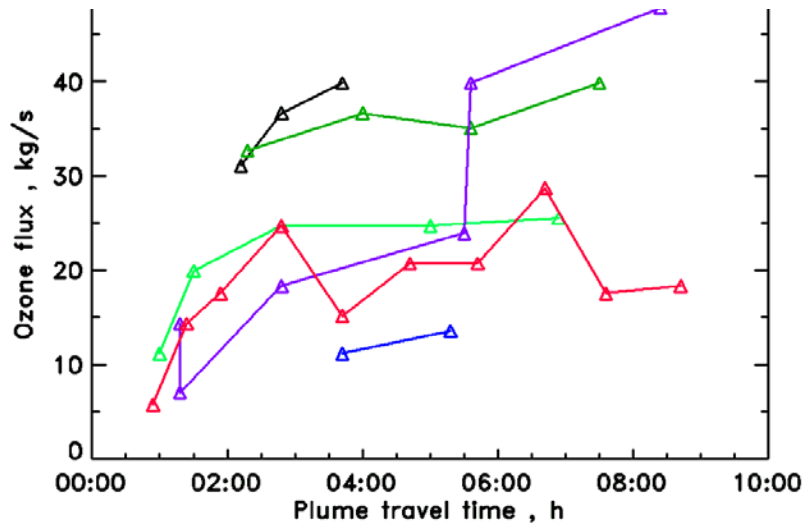
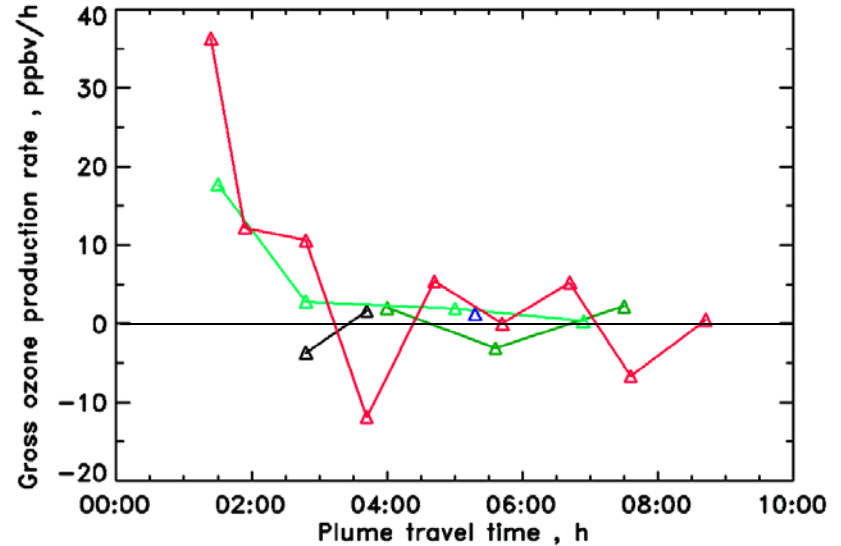
- Integrate excess ozone in plume (plume  $O_3$  – background  $O_3$ ).
- Multiply with horizontal wind speed (from wind profiler network) to yield ozone flux for each transect.

# Six Houston/Dallas ozone export cases studied

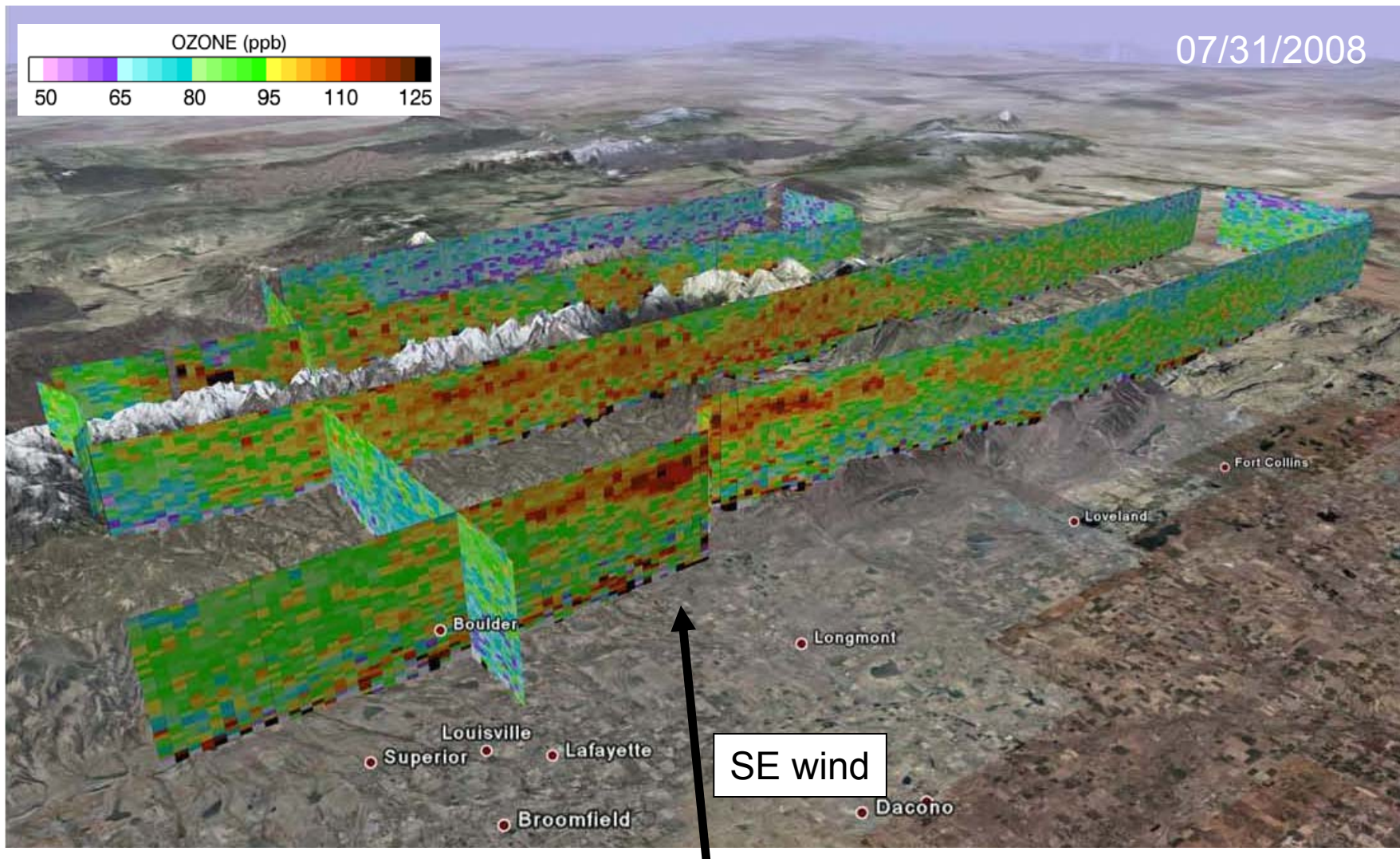


# Horizontal ozone flux and ozone production

A flux of  $35 \text{ kg O}_3 / \text{s}$  (average of all Houston cases) emitted over a day (8 hours) is equivalent to a 10-ppb increase in ozone over an approx. 10,000 square mile area, assuming a 2-km deep mixed layer.

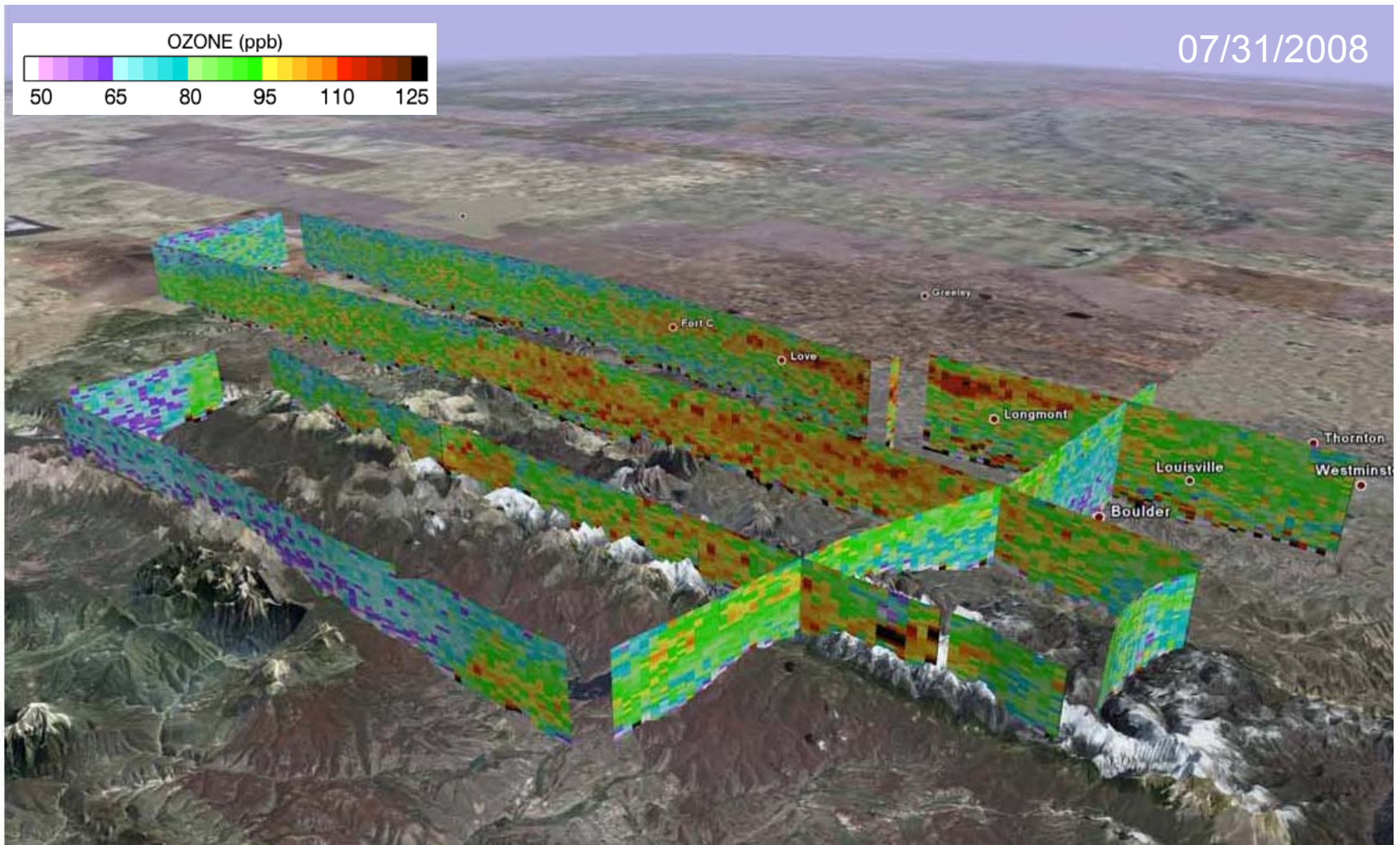


# Front Range Air Quality Study 2008: Transport of O<sub>3</sub> into and over the mountains





# Front Range Air Quality Study 2008: Transport of O<sub>3</sub> into and over the mountains (cont'd)



# Selected References (1)

---

## DIAL history (slides 5 - 6)

Schotland, R. M., 1974: Errors in the Lidar Measurement of Atmospheric Gases by Differential Absorption, *J. Appl. Meteorol.*, **13**, 71-77.

Shumate, M. S., R. T. Menzies, W. B. Grant, and D. S. McDougal, 1981: Laser Absorption Spectrometer: Remote Measurement of Tropospheric Ozone, *Appl. Opt.*, **20**, 545-553.

Pelon, J. and G. Megie, 1982: Ozone Monitoring in the Troposphere and Lower Stratosphere: Evaluation and Operation of a Ground-Based Lidar Station, *J. Geophys. Res.*, **87**, 4947-4955.

Megie, G. J., G. Ancellet, and J. Pelon, 1985: Lidar Measurements of Ozone Vertical Profiles, *Appl. Opt.*, **24**, 3454-3463.

Browell, E. V., S. Ismail, W. B. Grant, 1998: Differential Absorption Lidar (DIAL) Measurements from Air and Space, *Appl. Phys. B*, **67**, 399 – 410.

Ismail, S., E. V. Browell, R. A. Ferrare, S. A. Kooi, M. B. Clayton, V. G. Brackett and P. B. Russell, 2000: LASE Measurements of Aerosol and Water Vapor Profiles During TARFOX, *J. Geophys. Res.*, **105**, D8, 9903-9916.

## How to choose a DIAL absorption line? (slide 9)

Remsberg, E. E. and L. L. Gordley, 1978: Analysis of Differential Absorption Lidar from the Space Shuttle, *Appl. Opt.*, **17**, 624-630.

## DIAL transmitters (slide 13)

Fix, A., M. Wirth, A. Meister, G. Ehret, M. Pesch, and D. Weidauer, 2002: Tunable Ultraviolet Optical Parametric Oscillator for Differential Absorption Lidar Measurements of Tropospheric Ozone, *Appl. Phys. B*, **75**, 153 – 163.

## Selected References (2)

---

### DIAL transmitters (slide 13) – cont'd

Poberaj, G., A. Fix, A. Assion, M. Wirth, C. Kiemle, G. Ehret, 2002: Airborne All-solid-state DIAL for Water Vapour Measurements in the Tropopause Region: System Description and Assessment of Accuracy, *Appl. Phys. B*, **75**, 165 – 172.

Gibert, F. P. H. Flamant, D. Bruneau, and C. Loth, 2006: Two-micrometer Heterodyne Differential Absorption Lidar Measurements of the Atmospheric CO<sub>2</sub> Mixing Ratio in the Boundary Layer, *Appl. Opt.*, **45**, 4448-4458.

### NOAA/ESRL/CSD DIAL systems (slides 15 - 20)

Machol, J. L., T. Ayers, K. T. Schwenz, K. W. Koenig, R. M. Hardesty, C. J. Senff, M. A. Krainak, J. B. Abshire, H. E. Bravo, and S. P. Sandberg, 2004: Preliminary Measurements with an Automated Compact Differential Absorption Lidar for Profiling Water Vapor. *Appl. Opt.*, **43**, 3110-3121.

Alvarez II, R. J., W. A. Brewer, D. C. Law, J. L. Machol, R. D. Marchbanks, S. P. Sandberg, C. J. Senff, A. M. Weickmann, 2008: Development and Application of the TOPAZ Airborne Lidar System by the NOAA Earth System Research Laboratory, Proceedings of *24th International Laser Radar Conference*, Boulder, Colorado, USA, 23-27 June, 2008, 68-71.

### Aerosol correction & DUAL-DIAL (slides 21 - 22)

Browell, E. V., S. Ismail, and S. T. Shipley, 1985: Ultraviolet DIAL measurements of O<sub>3</sub> profiles in regions of spatially inhomogeneous aerosols, *Appl. Opt.*, **24**, 2827-2836.

Wang, Z., H. Nakane, H. Hu, and J. Zhou, 1997: Three-Wavelength Dual Differential Absorption Lidar Method for Stratospheric Ozone Measurements in the Presence of Volcanic Aerosols, *Appl. Opt.*, **36**, 1245-1252.